

# Cumulative Human impacts on Coral Reefs: Assessing Risk and Management Implications for Brazilian Coral Reefs

## S1. Details on each Stressor

### 1.1. Fishing

A fishing index was derived from mapping methods developed by [1], where the potential exposure to traditional and industrial fisheries were calculated according to Eq. (1) and (2), respectively, below. Google Earth Pro was used to map out a gradient of exposure of reef cells to fisheries by identifying and mapping the spatial locations of 3,610 traditional and 65 industrial active vessels in 429 fishing ports or fish landing sites throughout study region. Fishing vessels were placed in traditional and industrial categories according to their length; traditional vessels were typically 6–12 m long while industrial ones were > 15m. We allowed some flexibility in those values due to regional differentiation in fleet characteristics, following fishery reports [2–4]. Paddled canoes (typically <5 m) identified inside estuaries were excluded from the analyses because this simple technology restricts access to coral reefs. To define the maximum distance at which reef cells were deemed not to be fished by traditional vessels, we used a varying linear decay model in accordance with the location of the fishing port as reported by [35–37]. This maximum distance varied from 60 to 180 km offshore.

$$F_T = \sum_{i=1}^{426} f d_{Ti} \times (P_{Ti} \times B_T) \quad (1)$$

where potential exposure to the traditional fishery  $F_T$  is a function of  $f d_{Ti}$ , a distance decay factor (0–1) derived from the minimum at sea distance from the centroid of a reef cell to the  $i$ th port;  $P_{Ti}$ , the number of traditional vessels in the  $i$ th port;  $B_T$ , the difference in visual sampling efficiency of the traditional sector; and 426 represents the total number of fishing ports or fishing land sites relative to the artisanal fleet.  $B_T$  used here was 2.7 (i.e. the ratio between the number of vessels identified during fishing survey [4] – i.e. 9,600 – and the number of vessels identified through our survey – i.e. 3,610). The fishing intensity index for industrial fisheries is given by:

$$F_I = Z_I \left( \sum_{i=1}^{17} f d_{Ii} \times (P_{Ii} \times B_I \times E_I) \right) \quad (2)$$

where  $F_I$  is the potential exposure to the industrial fisheries;  $Z_I$  is the likely fishing use of a cell based on the depth of the cell;  $f d_{Ii}$ ,  $P_{Ii}$ ,  $B_I$  are the decay factor, number of vessels, and correction factor, respectively;  $E_I$  represents the efficiency of industrial vessels relative to traditional vessels as they differ in their amounts of fish caught; and 17 indicates the total number of fishing ports or fishing land sites relative to the industrial fleet. When calculating the potential exposure to industrial fisheries, the term  $Z_I$  in Eq. (2) was equal to 1 as data about the relationship between probabilities of industrial fishing occur and depth was not available. Similar to the artisanal fishery model, we allowed the linear decay model to be varied geographically and, in this case, the maximum distance in which a cell could be fished corresponded to the width of the continental shelf. As 200 industrial vessels are registered for the region [4], the ration between 200 and the number of vessels identified through our survey ( $B_I$ ) is equal to 3.07. Based on the best statistics on fishery landing available [5], we estimated  $E_I$  to be 14.2.

Our total reef fishing index **FII** was calculated by summing up both artisanal and industrial fishery intensities, and normalising the resulting values to a range of 0 to 1 (Eq. 3), where the value of 1 has the highest fishing exposure and 0 indicates cells under the lowest fishing exposure.

$$FII = \frac{[(F_T + F_I) - (F_T + F_I)_{\min}]}{(F_T + F_I)_{\max} - (F_T + F_I)_{\min}} \quad (3)$$

where  $(F_T + F_I)_{\max}$  and  $(F_T + F_I)_{\min}$  are the maximum and minimum combined scores for a reef cell in our study region, respectively. Our fishing index constitutes to date the most spatially coherent assessment of this stressor over such a large area.

### 1.2. Land-based activities

A land-based activity index was derived to estimate potential sediment supply associated with conversion of vegetation to other land uses in coastal catchments and its influence in coastal waters. The exposure to land-based activities was measured through the human footprint score summed across pixels and summarized for each coastal catchment in our study area (n=32 catchments; 1,015,150 pixels of 1 × 1km). The human footprint score classifies pixels according to their level of experiencing an incursion of human pressures [6]. We delineated coastal catchments based on 15 arc-sec HydroBasins (<http://www.hydrosheds.org/page/hydrobasins>) data. We then summarised the human footprint score within each catchment, based on land-use data, infrastructure, and human access to natural areas on the terrestrial environment for 2009 [7] and summed scores across pixels as the area of each catchment might also influence the amount of pollutants discharged into the ocean. The final component was intended to quantify the influence of land use on sedimentation of coastal waters. We thus allocated reef cells to the influence of specific rivers with the aid of remote sensing data. Landsat-5 satellite imagery, at a scale 1:50000, was used to delimit river plume influence in coastal waters associated with main rivers of the 32 catchments based on visual interpretation of the images over multi-temporal scales (2009-2011). For those reef cells subjected to river-plume influence, we then calculated the Euclidean distance from their centroid to the nearest river mouth. The final exposure to land-based activities was then calculated as Eq. 4 below:

$$LAI = fd_{Ri} \times HFI_{Li} \quad (4)$$

where **LAI** is the final exposure of a given reef cell to land-based activities,  $fd_{Ri}$  is the decay function (0-1) described by the Euclidean distance from each reef cell centroid to mouth of the nearest main river, and  $HFI_{Li}$  is the summed human footprint score associated with the respective catchment of the main river. Although this is an indirect measure of terrestrial sediment runoff and sediment delivery to the ocean, we lacked river discharge and plume dispersion modelling for our study area that could be used for a better understanding of the relationship between land activities and pollution supply. Using Eq. 5, below, the exposure value was then scaled from 0 (cells considered to be free of influence of river plumes) to 1 (cells at the closest distance to river mouths from catchments that have experienced high level of conversion of natural areas to human uses), as Eq. 5 below:

$$LAI = \frac{[(LAI) - (LAI)_{\min}]}{(LAI)_{\max} - (LAI)_{\min}} \quad (5)$$

where **LAI** is the **LAI** calculated for a given reef cell, and  $(LAI)_{\max}$  and  $(LAI)_{\min}$  are the maximum and minimum scores reported for any reef cell, respectively.

### 1.3. Coastal development

The coastal development index was calculated as originally proposed by [11]. The index is measured by a distance from night time lights emission provided by the Defense Meteorological Satellite Program (DMSP/NOAA). Night time lights represent a direct stressor to coral reef ecosystems (e.g. affecting coral spawning) and are an excellent proxy measure for disturbances associated with reduced coastal water quality, habitat modification caused by coastal engineering, and general uses of the shore [11]. The index is based on the metric LPI (light proximity index) that assumes a greater exposure to disturbances can be expected for reefs situated in close proximity to a

source of high night light intensity, than those found further away [1]. Similar to [1], we ran a sensitivity analyses to assess how results changed when using different input radii as the maximum distance from the centroid of a given reef cell. Because we found no significant differences when using distances further than 25 km, we used this threshold as the maximum distance to which a given reef would be exposed to our coastal development index **CDI** (Eq. 6). **CDI** was also scaled from 0 to 1 where a reef cell with a value of 0 means no light measured within 25 km and 1 means the most intense light affecting that cell.

$$CDI = \frac{[(LPI) - (LPI)_{min}]}{(LPI)_{max} - (LPI)_{min}} \quad (6)$$

where LPI (light proximity index) is the LPI calculated for a given reef cell (as Eq. 6),  $(LPI)_{max}$  and  $(LPI)_{min}$  are the maximum and minimum scores reported for any reef cell, respectively.

$$LPI = \frac{\sum L_{1...n}}{\sum D_{1...n}} \quad (7)$$

where L1 is the intensity recorded in each pixel of the satellite imagery and D1 is a distance from that pixel to a given reef cell (centroid to centroid).

#### 1.4. Ocean mining

Exposure to pollution or habitat destruction associated with ocean mining (including oil and gas exploration) was defined by overlapping reef cells with locations of mining activity derived from government databases publicly available through Sigmine (<http://sigmine.dnpm.gov.br>) and Brazilian National Petroleum Agency (ANP, <http://anp.gov.br>). The presence of marine mining activity and its area of influence (defined by applying a 10km buffer around the location of each singular location) was assigned to each reef cell based on a layer containing all mining fields. We then used this layer as binary data and classified each reef cell as exposed (1) or not exposed (0) to mining activities **OMI**.

#### 1.5. Aquaculture

We included data on aquaculture (shrimp farming) because it represents an important source of organic and inorganic pollution along the Brazilian northeastern coast and it has a great potential for future expansion [12]. The exposure to aquaculture-related disturbances was quantified by a Euclidean-distance-based model in which stress declines as distance to shrimp farms increases. Shrimp farm locations were mapped by [13] between 2007 and 2009. To model the exposure to this stressor, we calculated a decay function from each shrimp farm to the centroid of each reef cell with a maximum threshold of 25km set as a limit to the influence of a given farm on adjacent waters (similar to our coastal development index). We recognized that ocean currents can play a significant role by dispersing pollutants from this stressor, but small-scale coastal modelling is currently unavailable for our study area. We applied the decay function (Eq. 8) from the centroid of each farm pond (n=115) that would potentially affect a given reef cell (within a 25-km threshold) and scaled it from zero to one, as other data layers (Eq. 9).

$$ADI = \sum_{i=1}^{115} f d_{Ai} \quad (8)$$

where **ADI** is the potential exposure to the shrimp farm activities;  $f d_{Ai}$ , is the decay factor (0-1).

$$ADI = \frac{[(ADI) - (ADI)_{min}]}{(ADI)_{max} - (ADI)_{min}} \quad (9)$$

where **ADI** is the exposure calculated for a given reef cell (as Eq. 8),  $(ADI)_{max}$  and  $(ADI)_{min}$  are the maximum and minimum scores reported for any reef cell, respectively

### 1.6. Shipping movements

Shipping activity including domestic and international fleet and several vessel types (cargo vessels, oil tankers, container ships, and gas carriers) was recorded by AIS and made available by Marine Traffic (<https://www.marinetraffic.com>). This platform also reconstructs the ship tracks and estimates the resulting network density of cargo ship movements based on data accumulating ship positions over time (from 2015 to 2016). The density map was then used as a proxy for shipping-associated disturbances such as sediment resuspension and noise pollution. The density map was originally classified in four levels of ship movement: low, medium, high, and very high. We then converted these classes into the following levels of exposure, respectively: 0; 0.33; 0.66; and 1. We intersected the density map with reef cells to assign any of those values to all reef cells as a proxy of exposure to shipping movements (**SMI**). As this index is categorical, no normalization was required.

### 1.7. Thermal stress

Estimates of past thermal stress (1985-2009) were combined to create a layer representing the rate of sea-surface temperature rise. The rate of warming was calculated by applying nonlinear mixed effect modelling to monthly mean sea-surface temperature data (obtained from NOAA - <http://pathfinder.nodc.noaa.gov>). Further details on modelling the rate of warming can be found in [14]. The thermal stress index **TSI** is calculated according to Eq. (9) to be:

$$\mathbf{TSI} = \frac{[(\mathbf{TSI}) - (\mathbf{TSI})_{\min}]}{(\mathbf{TSI})_{\max} - (\mathbf{TSI})_{\min}} \quad (9)$$

where **TSI** is the the warming trend (°C decade) detected in each reef cell,  $(\mathbf{TSI})_{\max}$  and  $(\mathbf{TSI})_{\min}$  are the maximum and minimum scores reported for any reef cell, respectively

## S2. Additional Results

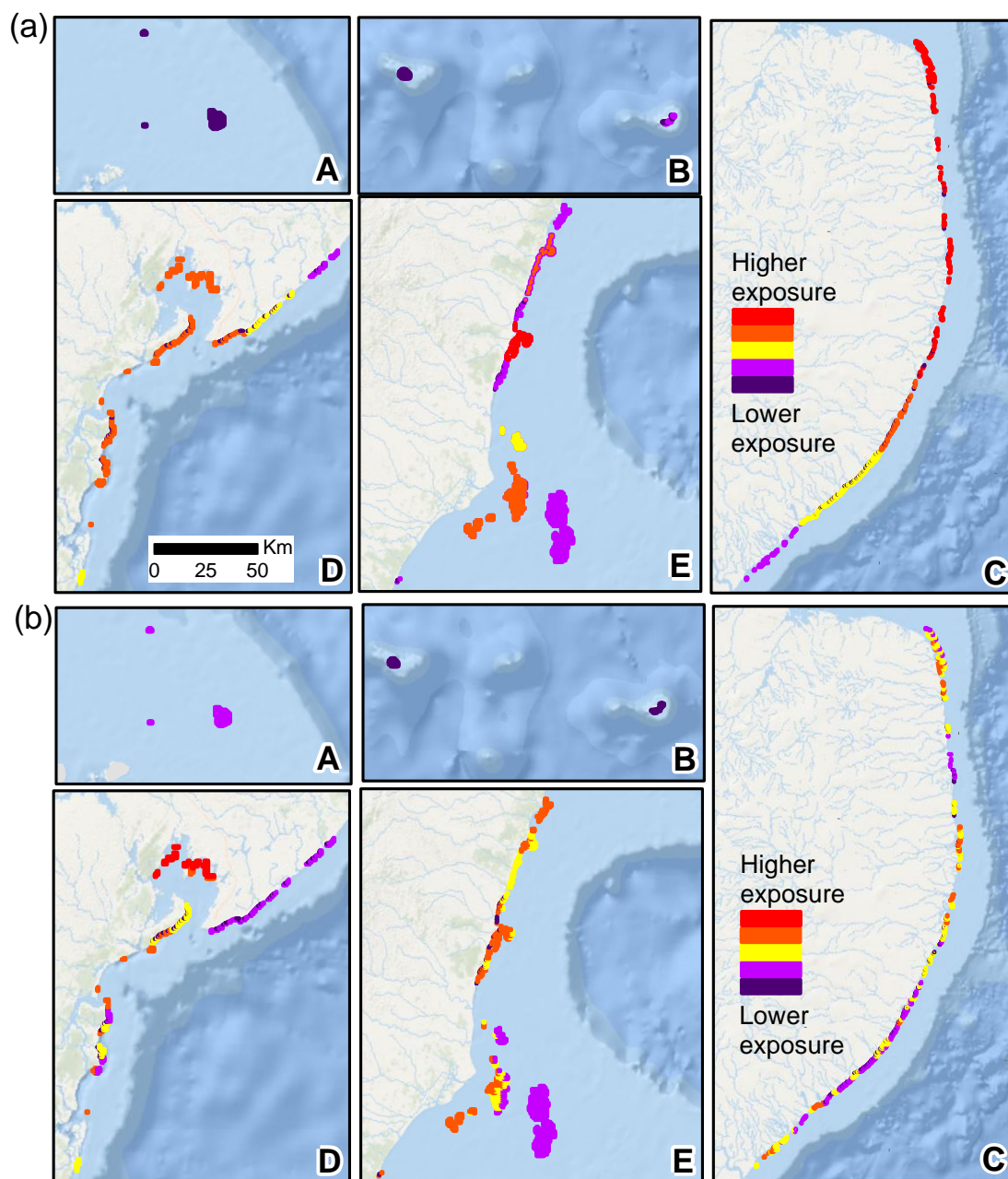


**Figure S1.** Spatial pattern of potential exposure to fishing (a) and land-based activities (b). Panels for reef cells within A-E sectors of the study area correspond to locations presented in Figure 1.

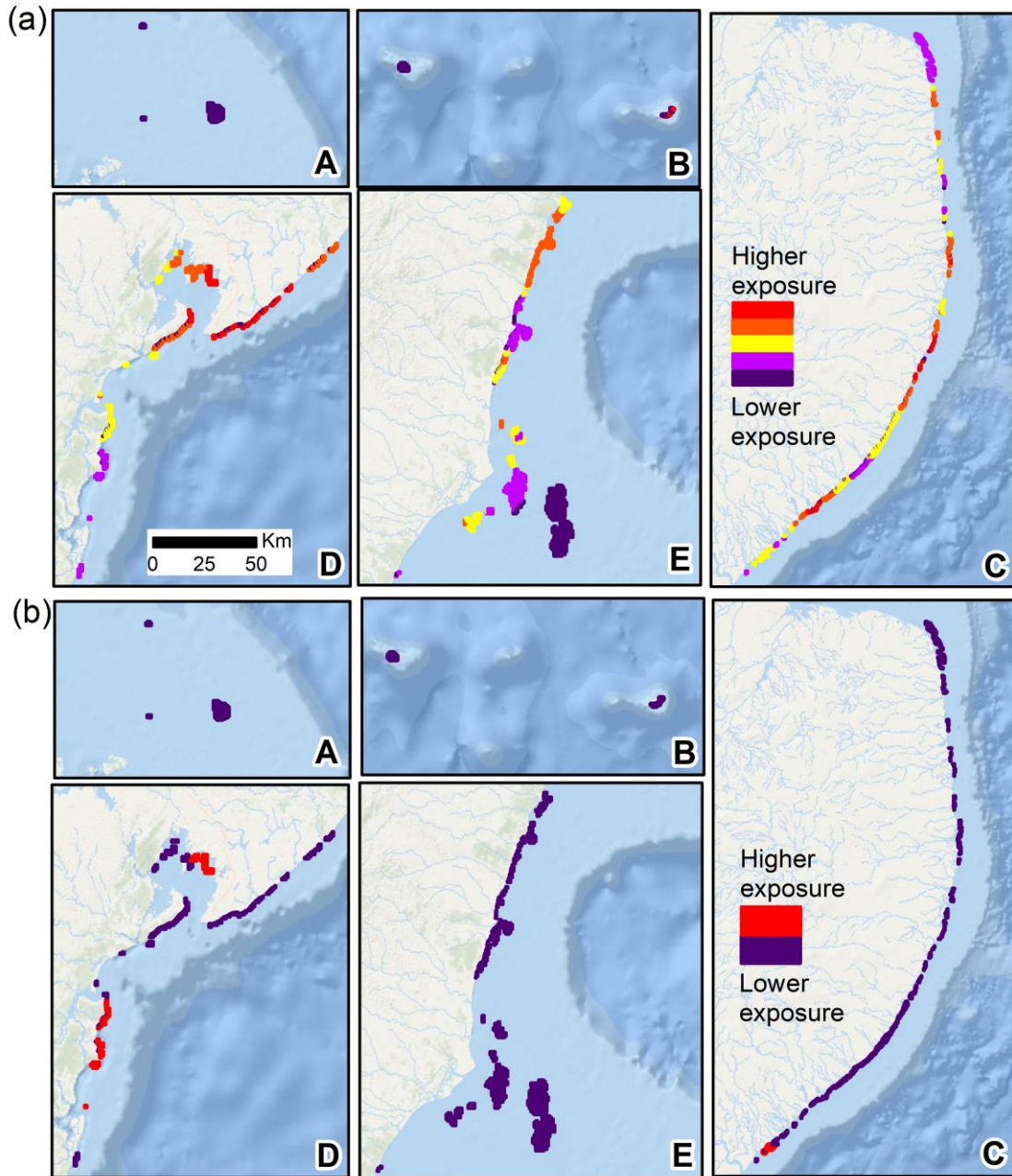


**Figure S2.** Spatial pattern of potential exposure to coastal development (a) and ocean mining (b). Panels for reef cells within A-E sectors of the study area correspond to locations presented in Figure 1.

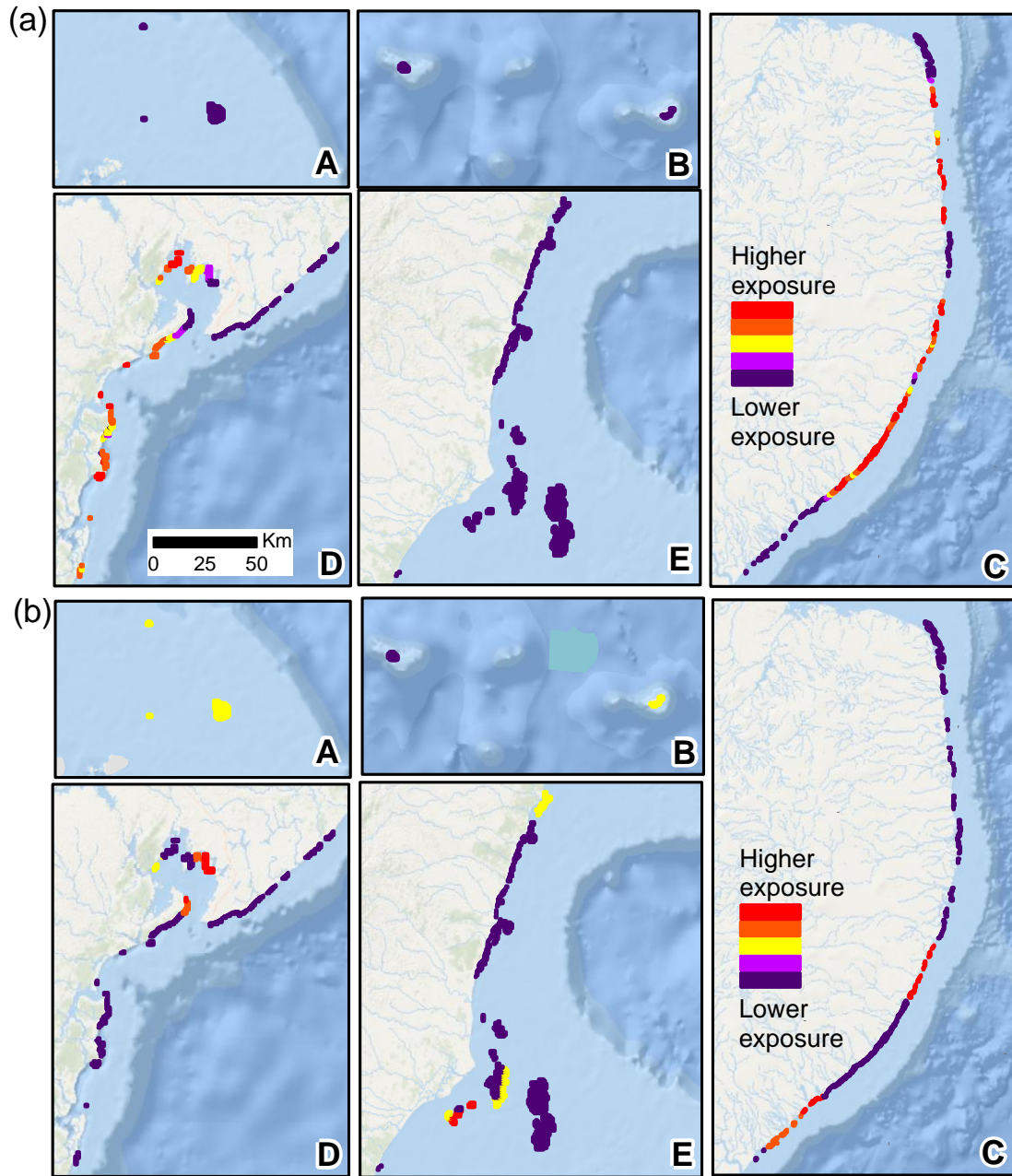


**Figure S3.** Spatial pattern of potential exposure to aquaculture (shrimp farming) (a) and shipping movements (b). Panels for reef cells within A-E sectors of the study area correspond to locations presented in Figure 1.

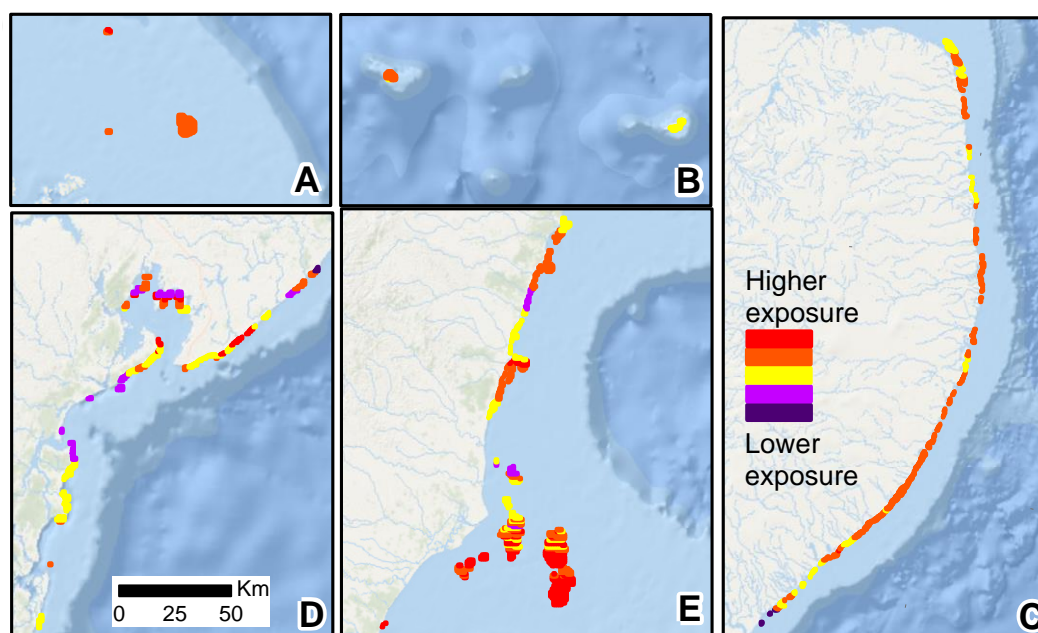


**Figure S4.** Spatial pattern of potential exposure to thermal stress. Panels for reef cells within A-E sectors of the study area correspond to locations presented in Figure 1.

## References

- Rowlands, G.; Purkis, S.; Riegl, B.; Metsamaa, L.; Bruckner, A.; Renaud, P. Satellite imaging coral reef resilience at regional scale. A case-study from Saudi Arabia. *Marine Pollution Bulletin* **2012**, *64*, 1222-1237.
- Brasil. Dinâmica de populações e avaliação de estoques dos recursos pesqueiros da região nordeste. FUNDAÇÃO DE AMPARO À PESQUISA DE RECURSOS VIVOS NA ZONA ECONÔMICA EXCLUSIVA – FUNDAÇÃO PROZEE: 2004; p 288.
- Brasil. *Relatório técnico do projeto de cadastramento das embarcações pesqueiras no litoral das regiões norte e nordeste do Brasil*; 2005; p 288.
- Brasil. *Monitoramento da atividade pesqueira no litoral nordestino – projeto estatpesca*; 2008; p 384.
- Brasil. Boletim estatístico da pesca e aquicultura. Ministério de Estado da Pesca e Aquicultura – MPA: 2010; p 129.
- Venter, O.; Sanderson, E.W.; Magrath, A.; Allan, J.R.; Beher, J.; Jones, K.R.; Possingham, H.P.; Laurance, W.F.; Wood, P.; Fekete, B.M. Sixteen years of change in the global terrestrial human footprint and implications for biodiversity conservation. *Nature communications* **2016**, *7*.
- Venter, O.; Sanderson, E.W.; Magrath, A.; Allan, J.R.; Beher, J.; Jones, K.R.; Possingham, H.P.; Laurance, W.F.; Wood, P.; Fekete, B.M. Global terrestrial human footprint maps for 1993 and 2009. *Scientific data* **2016**, *3*, sdata201667.
- Hoskins, A.J.; Bush, A.; Gilmore, J.; Harwood, T.; Hudson, L.N.; Ware, C.; Williams, K.J.; Ferrier, S. Downscaling land-use data to provide global 30 " estimates of five land-use classes. *Ecology and Evolution* **2016**, *6*, 3040-3055.
- Atlas dos remanescentes florestais da mata atlântica – período de 2011-2012. INPE, S.M.A., Ed. Fundação SOS Mata Atlântica; São Paulo, 2012.
- Atlas dos remanescentes florestais da mata atlântica - 2007-2008. INPE, S.M.A., Ed. Fundação SOS Mata Atlântica; São Paulo, 2008.
- Aubrecht, C.; Elvidge, C.; Longcore, T.; Rich, C.; Safran, J.; Strong, A.; Eakin, C.; Baugh, K.; Tuttle, B.; Howard, A. A global inventory of coral reef stressors based on satellite observed nighttime lights. *Geocarto International* **2008**, *23*, 467-479.
- Hatje, V.; de Souza, M.M.; Ribeiro, L.F.; Eca, G.F.; Barros, F. Detection of environmental impacts of shrimp farming through multiple lines of evidence. *Environmental Pollution* **2016**, *219*, 672-684.
- Magris, R.A.; Barreto, R. Mapping and assessment of protection of mangrove habitats in Brazil. *Pan-Am J Aquat Sci* **2010**, *5*, 546-556.

14. Magris, R.; Heron, S.F.; Pressey, R.L. Conservation planning for coral reefs accounting for climate warming disturbances. *PLoS One* **2015**.



© 2018 by the authors. Submitted for possible open access publication under the terms and conditions of the Creative Commons Attribution (CC BY) license (<http://creativecommons.org/licenses/by/4.0/>).